Cover Sheet

This is a preprint. This paper is currently under peer-review at the Journal of Atmospheric Pollution Research (ISSN: 1309-1042). We welcome feedback and invite you to contact the authors directly to comment on the manuscript (shithi0914@student.nstu.edu.bd).

Authors

Shithi Dhar Bristy, e-mail: shithi0914@student.nstu.edu.bd; https://orcid.org/0009-0008-1422-5514

Md Lokman Hossain, e-mail: lokmanbbd@gmail.com; https://orcid.org/0000-0002-6103-4226

Md. Sabbir Ahmed Ruman, e-mail: sabbiresdmnstu@gmail.com; https://orcid.org/0009-0001-0529-4349

Jannat Binte Jalal, e-mail: jannat0912@student.nstu.edu.bd; https://orcid.org/0009-0004-9820-5967

Derrick Y.F. Lai, e-mail: dyflai@cuhk.edu.hk; https://orcid.org/0000-0002-1225-9904

Corresponding author: Shithi Dhar Bristy, e-mail: shithi0914@student.nstu.edu.bd

Spatiotemporal dynamics of air pollution and vegetation health in a rapidly urbanizing city in northeastern Bangladesh

Shithi Dhar Bristy[1*], Md Lokman Hossain[2], Md. Sabbir Ahmed Ruman[1], Jannat Binte Jalal[1], Derrick Y.F. Lai[2], Pinaki Chowdhury[1]

[1]Department of Environmental Science and Disaster Management, Noakhali Science and Technology University, Noakhali, Bangladesh
[2]Department of Geography and Resource Management, The Chinese University of Hong Kong, New Territories, Hong Kong

Shithi Dhar Bristy, e-mail: shithi0914@student.nstu.edu.bd; https://orcid.org/0009-0008-1422-5514
Md Lokman Hossain, e-mail: lokmanbbd@gmail.com; https://orcid.org/0000-0002-6103-4226
Md. Sabbir Ahmed Ruman, e-mail: sabbiresdmnstu@gmail.com; https://orcid.org/0009-0001-0529-4349
Jannat Binte Jalal, e-mail: jannat0912@student.nstu.edu.bd; https://orcid.org/0009-0004-9820-5967
Derrick Y.F. Lai, e-mail: dyflai@cuhk.edu.hk; https://orcid.org/0000-0002-1225-9904
Pinaki Chowdhury, e-mail: pinaki.esdm@nstu.edu.bd; https://orcid.org/0000-0001-7204-2400
***Corresponding author's email:** Shithi Dhar Bristy, e-mail: shithi0914@student.nstu.edu.bd; https://orcid.org/0009-0008-1422-5514

Abstract

Air pollution poses a significant environmental concern and is recognized as the fourth leading risk factor affecting human health. Understanding the levels of air pollution and its relationships with vegetation is crucial for assessing health risks under rapid urbanization. In this study, using the extracted imagery from the Sentinel-5 and Moderate Resolution Imaging Spectroradiometer (MODIS) satellites for the period 2019-2023, five key pollutants, including ozone (O_3), sulfur dioxide (SO_2), carbon monoxide (CO), nitrogen dioxide (NO_2), and particulate matter ($PM_{2.5}$), along with normalized difference vegetation index (NDVI), were processed to analyze the monthly, seasonal, and annual patterns of these variables in a rapidly growing city in northeastern Bangladesh. Monthly and seasonal variations in the concentrations of O_3, NO_2, $PM_{2.5}$, and CO showed significant differences, while annual variations for these pollutants were not significant. NO_2 concentrations were highest during winter (85.7 µmol m^{-2}), while the highest concentrations of CO (0.047 mol m^{-2}), O_3 (0.127 mol m^{-2}), SO_2 (137 µmol m^{-2}), and $PM_{2.5}$ (40.74 µg/m^3) were observed during the pre-monsoon season. Spatial variations were also recorded for these pollutants, with higher NO_2 concentrations in the eastern part and elevated SO_2 and $PM_{2.5}$ in the southern part. Expectedly, the highest NDVI values were recorded during the post-monsoon (0.66), while the lowest occurred during the winter (0.48). The northeastern region consistently exhibited higher vegetation greenness. NDVI showed a negative correlation with the five air pollutants studied, with significant negative correlations observed between NDVI and NO_2, and between NDVI and $PM_{2.5}$. Conversely, the positive correlations among the air pollutants (albeit not all were statistically significant) suggest possible shared sources or overlapping emission patterns. This study highlights the urgent necessity for targeted air quality management and urban greening

initiatives to mitigate the adverse effects of air pollution on vegetation functioning and promote sustainable development in rapidly urbanizing cities.

Keywords: Air pollutants; Carbon monoxide; NDVI; Ozone; Urbanization; Vegetation greenness

Introduction

Air pollution is a significant global challenge, both environmentally and in terms of public health (Liu *et al.*, 2021). It is identified as the fourth leading risk factor affecting human health (Wei *et al.*, 2023) and is responsible for over 4 million premature deaths annually (Shaddick *et al*., 2020). According to the Global Burden of Disease study, air pollution was responsible for approximately 6.7 million deaths worldwide in 2019, underscoring its substantial impact on public health and mortality (Murray *et al*., 2020). This issue is particularly severe in rapidly urbanizing regions of developing countries, where industrial expansion and increased reliance on fossil fuels for industrial and residential activities have significantly worsened air quality (He *et al.*, 2017). These activities emit hazardous substances, including gases (e.g., carbon monoxide [CO], nitrogen oxides [NO_X]) and particulate matter (e.g., $PM_{2.5}$, PM_{10}), into the atmosphere, further contributing to environmental degradation and public health risks (Kampa and Castanas, 2008; Hou *et al*., 2019).

Major urban areas are heavily polluted with harmful substances such as CO, ozone (O_3), sulfur dioxide (SO_2), NO_X, $PM_{2.5}$, and PM_{10}. These pollutants significantly degrade environmental quality and pose severe risks to human health (Zhang *et al.*, 2020). The Air Quality Index (AQI) is directly associated with health risks, including respiratory and cardiovascular complications (like asthma and heart attacks) (Liu, 2002; Eckhoff, 2009). Studies have consistently demonstrated that exposure to air pollution, whether short-term or long-term, is linked to a rise in cardiac-related deaths and hospitalizations for respiratory illnesses. Outdoor air pollution alone is responsible for approximately 4.2 million deaths annually, with the majority occurring in densely populated urban areas dominated by industrial activities, energy production, and automobile traffic (WHO, 2019).

South Asia is one of the regions severely affected by urban air pollution, with over 250,000 deaths annually attributed to related health issues. Rapid urbanization in developing countries has led to much higher exposure levels, worsening the problem. In addition to harming human health, air pollution also affects vegetation. Plants exposed to polluted environments exhibit signs of damage, such as leaf injury and reduced growth, which pose significant threats to agriculture in these regions (Reig-Armiñana *et al.*, 2004; Tiwari *et al.*, 2012). Cities in Bangladesh, including Dhaka, Sylhet, and Chattogram, exhibit the world's worst air pollution levels. Dhaka, in particular, ranks among the most polluted cities in the world (Alam *et al.*, 2018). The country's rapid urbanization and industrial growth significantly contribute to the problem, underscoring the urgent need for mitigation strategies.

According to the World Bank, air pollution in Bangladesh, particularly from $PM_{2.5}$, poses a severe public health threat. Annual $PM_{2.5}$ levels range from 60–100 μg/m³ nationally and reach 90–100 μg/m³ in Dhaka, far exceeding the WHO's safe guideline of 5 μg/m³. Breathing air in Dhaka has been equated to smoking nearly two cigarettes daily (Das 2025). This pollution plays a significant role in premature mortality, being responsible for 55% of such deaths in Bangladesh. It also causes over 2.5 billion days of illness annually, costing the economy 8.32% of its

GDP in 2019 (Das 2025). These figures underscore the urgent need to address air pollution as a critical driver of health and economic crises in Bangladesh.

Reliable prediction and mitigation of air pollutants require continuous and accurate monitoring. Remote sensing techniques and geographic information systems (GIS) offer valuable tools for assessing air quality, especially in areas lacking ground-based monitoring stations (Guo *et al.*, 2019). For instance, the Normalized Difference Vegetation Index (NDVI), obtained from MODIS sensors, is a critical metric for measuring vegetation density and monitoring environmental changes (Guo *et al.* 2019; Hossain *et al.*, 2023). NDVI has proven useful for environmental management, helping to identify areas where vegetation is under stress due to environmental stresses (Kusuma *et al.*, 2019; Hossain and Li, 2021).

As urbanization accelerates in the northern region of Bangladesh, particularly in the Sylhet district, air pollution has become a growing concern. However, despite the increasing environmental challenges, there is a significant gap in research examining the relationship between air pollutants and vegetation greenness in the Sylhet Sadar Upazila (sub-district). Understanding this relationship is crucial because air pollution not only poses significant risks to human health but also adversely affects vegetation, which plays a vital role in maintaining ecological balance and mitigating environmental degradation.

This research seeks to analyze the spatiotemporal patterns of air pollutants and quantify their correlation with vegetation greenness using GIS and Google Earth Engine (GEE) over five years (2019-2023), providing critical insights into the environmental effects of air pollution in this region. By analyzing spatiotemporal trends in air pollutants and vegetation greenness over a five-year period using advanced tools (GIS and GEE), this research provides critical insights into how urbanization affects environmental quality. The findings help address the lack of region-specific data, inform policies for air quality management, and support sustainable urban planning efforts in Sylhet, where balancing development and environmental conservation is increasingly important.

Methodology

Study area background

This study area encompasses the Sylhet Sadar sub-district (upazila) in the Sylhet district, located in northeastern Bangladesh (Fig. 1). The study area is bordered by Jaintiapur, Gowainghat, and Companiganj sub-districts to the north, Dakshin Surma sub-district to the south, Golapganj and Kanaighat sub-districts to the east, and Chhatak (in the Sunamganj district) and Bishwanath sub-district to the west. The selected sub-district comprises eight unions (Fig. 1). The presence of unique features, including hills, plateaus, tea plantations, woodlands, watercourses, and religious sites, distinguishes it from other sub-districts in Bangladesh.

According to the 2011 National Census, the selected area has a population of approximately 487,000, residing in around 98,000 households. Despite the average yearly population growth rate of 2.1% from 2001 to 2011 being lower than in previous decades, it still surpassed the national growth rate of 1.2% over the same period. The literacy rate in Sylhet has steadily increased over the years, rising from 37.9% in 1981 to 48.5% in 1991, 56.2% in 2001, and 63.4% in 2011. According to BBS (2021), the literacy rate of males (females) in 2011 was 59.1% (52.3%).

Sylhet Sadar Upazila experiences a tropical monsoon climate characterized by hot, humid summers and mild, dry winters. Summer temperatures range from 25 °C to 31 °C, while winter temperatures vary between 12 °C and 20 °C. The region receives annual rainfall between 3,334 mm and 4,200 mm, with approximately 80% of the total precipitation occurring during May and September (monsoon season). During this period, the prevailing winds come from the southeast, whereas the winter months experience northeasterly winds (BMD, 2025).

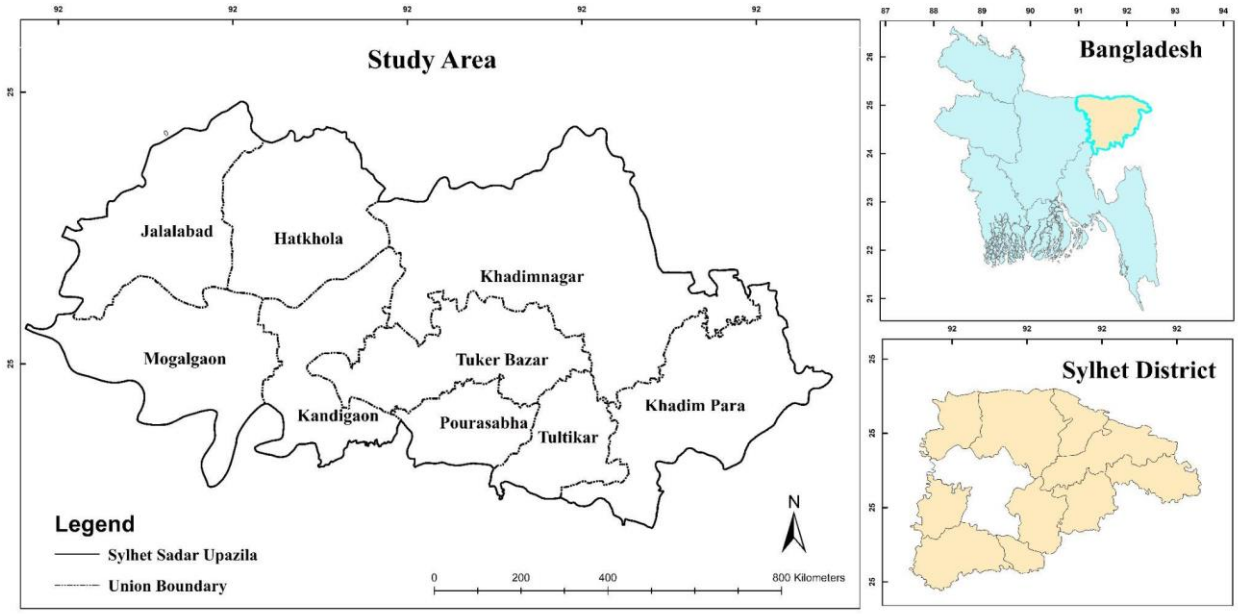

Fig. 1 The study location map shows the positions of eight selected unions in the studied sub-district (Sylhet Sadar) in the northeastern region of Bangladesh.

Data sources

For the period of 2019 to 2023, Remote sensing data from multiple high-resolution sources were collected (Table 1). These sources include atmospheric data from the Sentinel-5P satellite (TROPOMI instrument), MODIS sensors onboard the Terra and Aqua satellites, and vegetation indices datasets. Data for NO_2, SO_2, O_3, and CO were retrieved from the TROPOMI instrument onboard the Sentinel-5P satellite, provided by the European Space Agency (ESA). For $PM_{2.5}$ analysis, daily satellite images from the MODIS/006/MCD19A2_GRANULES dataset were used. These images, featuring a spatial resolution of 1 km, were accessed and processed using GEE. The MOD13Q1 version 006 dataset was utilized to analyze vegetation cover, which provides 16-day global vegetation indices at a 250 m resolution.

Table 1 Details of the datasets, including the name of pollutants and their descriptions (Source: Earth Engine Data Catalog)

Name of pollutant (unit)	Image name	Band name	Minimum (Maximum) value	Reference
NO_2 (mol m^{-2})	Sentinel-5P OFFL NO_2: Offline Nitrogen Dioxide	NO_2_column_number_density	−0.00051 (0.0192)	European Union/ESA/Copernicus Haque *et al.* 2022; Tuli *et al.* 2025
SO_2 (mol m^{-2})	Sentinel-5P OFFL SO_2: Offline Sulfur Dioxide	SO_2_column_number_density	−0.4051 (0.2079)	
O_3 (mol m^{-2})	Sentinel-5P OFFL O_3: Offline Ozone	O_3_column_number density	0.025 (0.3048)	
CO (mol m^{-2})	Sentinel-5P NRTI CO: Near Real-Time Carbon Monoxide	CO_column_number_density	−279 (4.64)	
AOD	MCD19A2.006: Terra & Aqua MAIAC Land Aerosol Optical Depth Daily 1 km	Optical_Depth_047	−100 (5000)	NASA LP DAAC at the USGS EROS Center

Data processing and analysis

Spatiotemporal analysis of air pollutant concentration

This study examined five major air pollutants: NO_2, SO_2, O_3, CO, and $PM_{2.5}$. GEE, an open-source geospatial analysis platform, was used to analyze these pollutants from 2019 to 2023. A custom web-based code in GEE was developed to collect and process remote sensing data for the selected pollutants.

Data for NO_2, SO_2, O_3, and CO were obtained from the TROPOMI instrument onboard the Sentinel-5P satellite, operated by the ESA. TROPOMI, a cutting-edge multispectral imaging spectrometer, is designed to operate across multiple wavelength ranges, including ultraviolet-visible (270–495 nm), near-infrared (675–775 nm), and shortwave-infrared (2305–2385 nm). Using passive remote sensing techniques, TROPOMI detects solar energy reflected from the Earth's surface, enabling the identification and measurement of specific atmospheric substances by capturing their unique signatures across the electromagnetic spectrum. For monitoring $PM_{2.5}$ within the study region (i.e., Sylhet sub-district), the Aerosol Optical Depth (AOD) data obtained from the MODIS onboard Terra and Aqua satellites were analyzed. To estimate $PM_{2.5,}$ AOD values were converted using a regression equation (Gupta *et al.*, 2018).

The images were preprocessed. After collecting and accessing the data, a JavaScript program was created within the GEE platform to streamline and automate the image analysis process. The shapefile of the study area was imported to define the geographical boundary. Once the remote sensing data were processed, the results were exported and imported into ArcMap 10.8 to visualize the spatial distribution of air quality and create a self-explanatory map (Fig. 2).

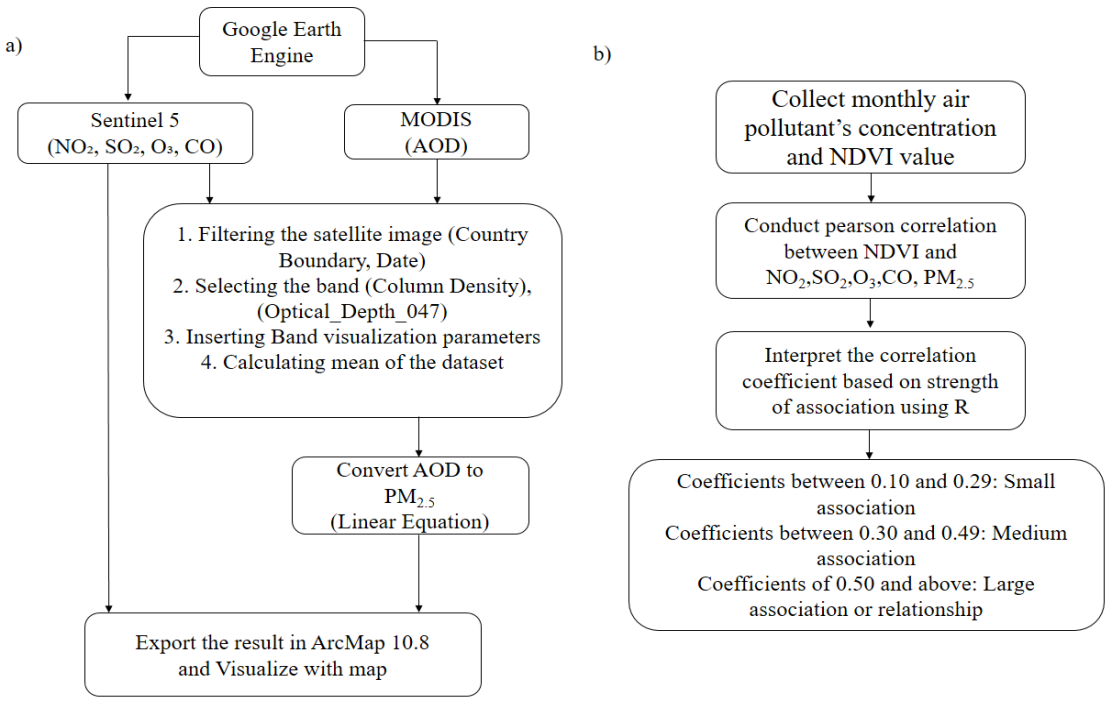

Fig. 2 Methodological flowchart (a) illustrating the data sources, processing, and analysis, and (b) quantifying the correlation between vegetation greenness (NDVI) and air pollutants.

Normalized difference vegetation index (NDVI)

NDVI is the ratio of the difference between the reflection value of the near-infrared (NIR) band and the reflection value of the red-light (RED) band in the remote sensing image.

$$NDVI = \frac{NIR - RED}{NIR + RED}$$

Monthly NDVI data of the highest quality and under cloud-free conditions were acquired using GEE for each union within Sylhet Sadar Upazila. The data were sourced from the MOD13Q1 (v006) Terra Vegetation Indices dataset, which provides 16-day global records at a 250-meter resolution, covering the period from 2019 to 2023.

Spatial distribution of air pollutants and vegetation greenness

Spatial distribution maps of the concentration of five air pollutants were generated employing interpolation methods to develop a continuous surface across the selected study region based on observed pollution values at specific locations. Zonal statistics were utilized to calculate the average value for the respective union. The average NDVI value and air pollution concentrations for each union were measured over a 60-month period from 2019 to 2023.

The inverse distance weighted (IDW) interpolation method was used to estimate unknown values at a particular location. This approach emphasizes the influence of nearby points, predicting the value of an unknown location based on the recorded values of surrounding known locations.

$$Z_p = \frac{\sum_{i=0}^{n}(\frac{Z_i}{d_i^p})}{\sum_{i=1}^{n}\frac{1}{d_i^p}}$$

Here, Z_p= value to be assessed, Z_i= known value, d_i^p = distance to a known point, n = exponent chosen by the user

Quantifying the association between vegetation greenness and air pollutants

Monthly union-level data provided a substantial sample size for examining the association between the five selected air pollutants and vegetation greenness. To establish a correlation between air pollutants and NDVI, monthly data for each pollutant and NDVI were collected at the union level for five years (2019-2023). The monthly concentrations of each air pollutant were tested against the corresponding monthly NDVI values for each union using the Pearson correlation test. This test quantified the strength (weak or strong) and direction (positive or negative) of the correlation between NDVI and the pollutants. In Pearson's correlation, coefficients between 0.10 and 0.29 represent a small association, coefficients between 0.30 and 0.49 represent a medium association, and coefficients of 0.50 and above represent a strong association.

Results

Air pollutants and vegetation greenness

NO_2 concentrations

The concentration of NO_2 showed distinct monthly, seasonal, and yearly patterns (Fig. 3). Significant differences in NO_2 concentration were observed for monthly (Fig. 3a, $p < 0.001$) and seasonal (Fig. 3b, $p < 0.001$) variations. In comparison, the differences in NO_2 concentration were not significant for annual changes (Fig. 3c, $p > 0.05$). Monthly data revealed that NO_2 concentrations were maximum in December (90.4 μmol m^{-2}) and minimum in October (63.8 μmol m^{-2}). Seasonally, NO_2 concentrations were highest during winter (85.7 μmol m^{-2}) and showed a decreasing trend through the pre-monsoon (77.4 μmol m^{-2}), monsoon (69.8 μmol m^{-2}), and post-monsoon (64 μmol m^{-2}). Yearly, the highest NO_2 concentration (78.2 μmol m^{-2}) was observed in 2023, while the lowest (70.9 μmol m^{-2}) was recorded in 2020 (Fig. 3c). When analyzing the spatial variation over the five study years, it became evident that NO_2 concentrations differed significantly across the various unions of the sub-district. The eastern part of the study area consistently exhibited higher NO_2 concentrations throughout the five years (Fig. 3d).

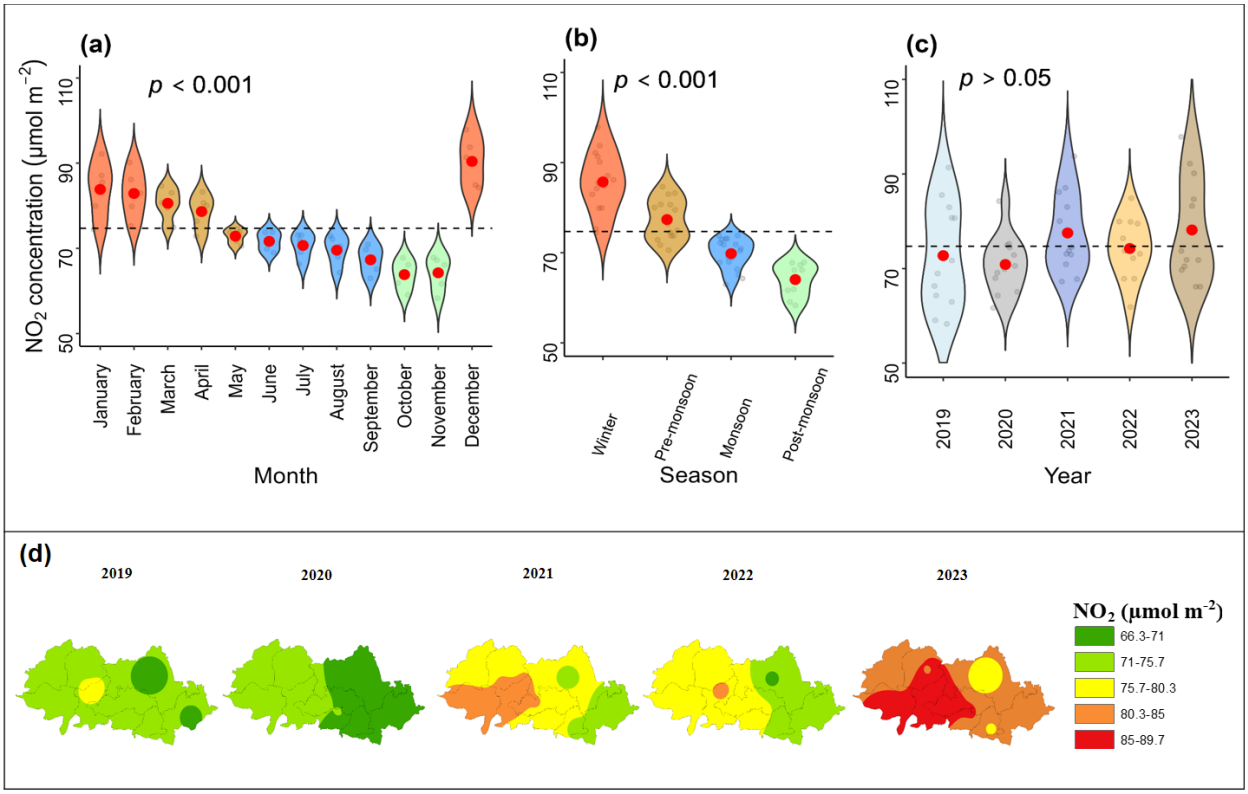

Fig. 3 Variations of NO_2 concentration for the respective months (**a**), seasons (**b**), years (**c**), and spatial patterns of NO_2 concentration (**d**) over the study area for the period 2019-2023. Points inside the violin plots are the NO_2 values. The red points inside the violin plots represent the mean NO_2 values. The dashed horizontal line indicates the base mean. The *p*-values have been obtained using a one-way ANOVA.

SO_2 concentrations

While monthly changes in SO_2 concentrations were not statistically significant (Fig. 4a, $p > 0.05$), seasonal (Fig. 4b, $p < 0.01$) and yearly (Fig. 4c, $p < 0.01$) changes showed significant variation. The highest SO_2 concentrations were observed in January (149 µmol m^{-2}) and the lowest in September (67 µmol m^{-2}). Seasonally, SO_2 concentrations peaked during the pre-monsoon period (137 µmol m-2), declined through the winter (129 µmol m-2), and then increased again during the post-monsoon period (105 µmol m-2), before decreasing further during the monsoon (79 µmol m^{-2}). Temporal patterns showed an increasing trend in SO_2 concentrations from 80 µmol m^{-2} in 2019 to 159 µmol m^{-2} in 2023 (Fig. 4c). Spatial patterns demonstrated that the southern zones usually exhibited elevated SO_2 levels, notably in 2020 and 2022 (Fig. 4d).

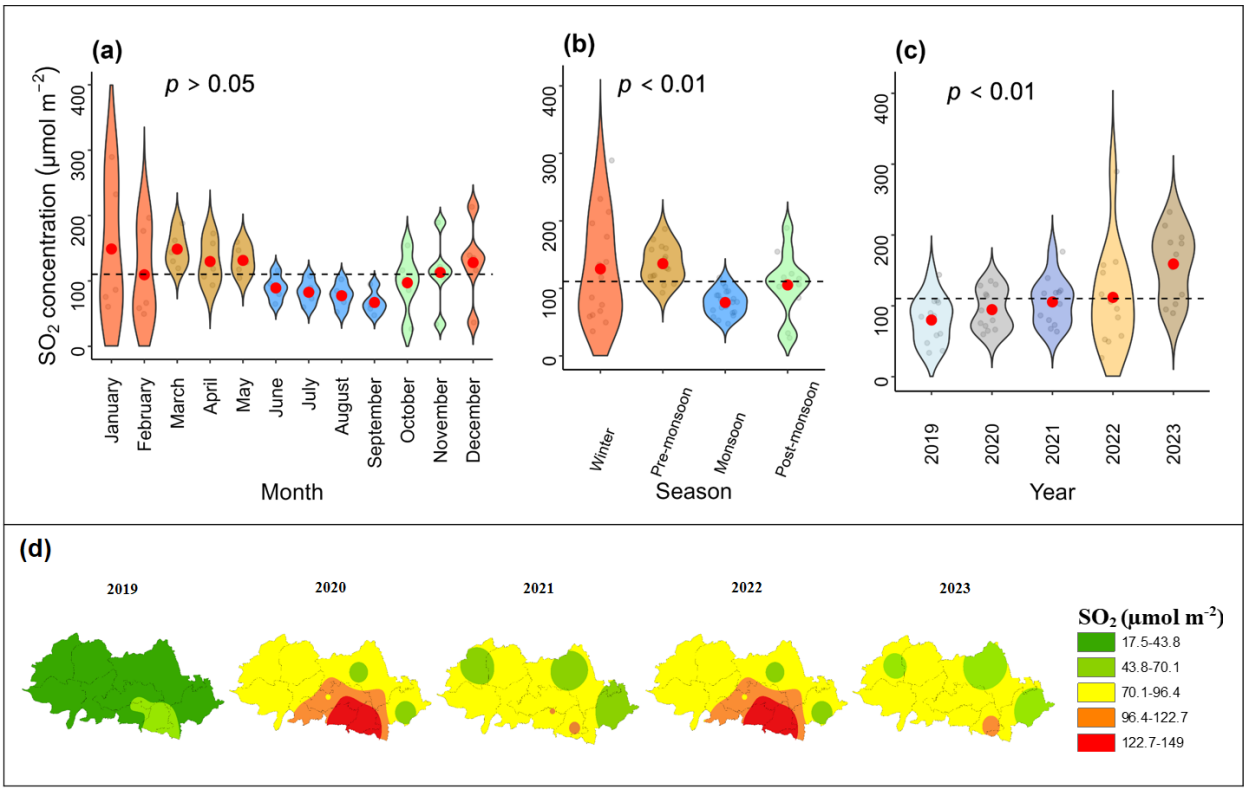

Fig. 4 Variations of SO_2 concentration for the respective months (**a**), seasons (**b**), years (**c**), and spatial patterns of SO_2 concentration (**d**) over the study area for the period 2019-2023. Figure descriptions are the same as those in Fig. 3, but for the SO_2 concentration.

CO concentrations

Similar to the NO_2 concentrations (Figs. 3a-c), significant differences in CO concentrations were observed for monthly (Fig. 5a) and seasonal (Fig. 5b) changes (both $p < 0.001$), while yearly variations were not significant (Fig. 5c, $p > 0.05$). CO concentrations were highest in March (0.049 mol m^{-2}) and lowest in July and August (0.033 mol m^{-2}). Seasonally, CO peaked during the pre-monsoon (0.047 mol m^{-2}) and reached its minimum during the monsoon (0.035 mol m^{-2}). No detectable patterns were observed for temporal variations in CO concentrations, which ranged between 0.040 mol m^{-2} in 2019 and 0.042 mol m^{-2} in 2021 (Fig. 5c). Over the five years, spatial patterns demonstrated that CO concentrations varied considerably across the unions of the sub-district (Fig. 5d). The lowest levels were observed in 2019 and 2022, mainly across the western and northern regions, while elevated concentrations appeared in 2021, particularly in the southern region (Fig. 5d).

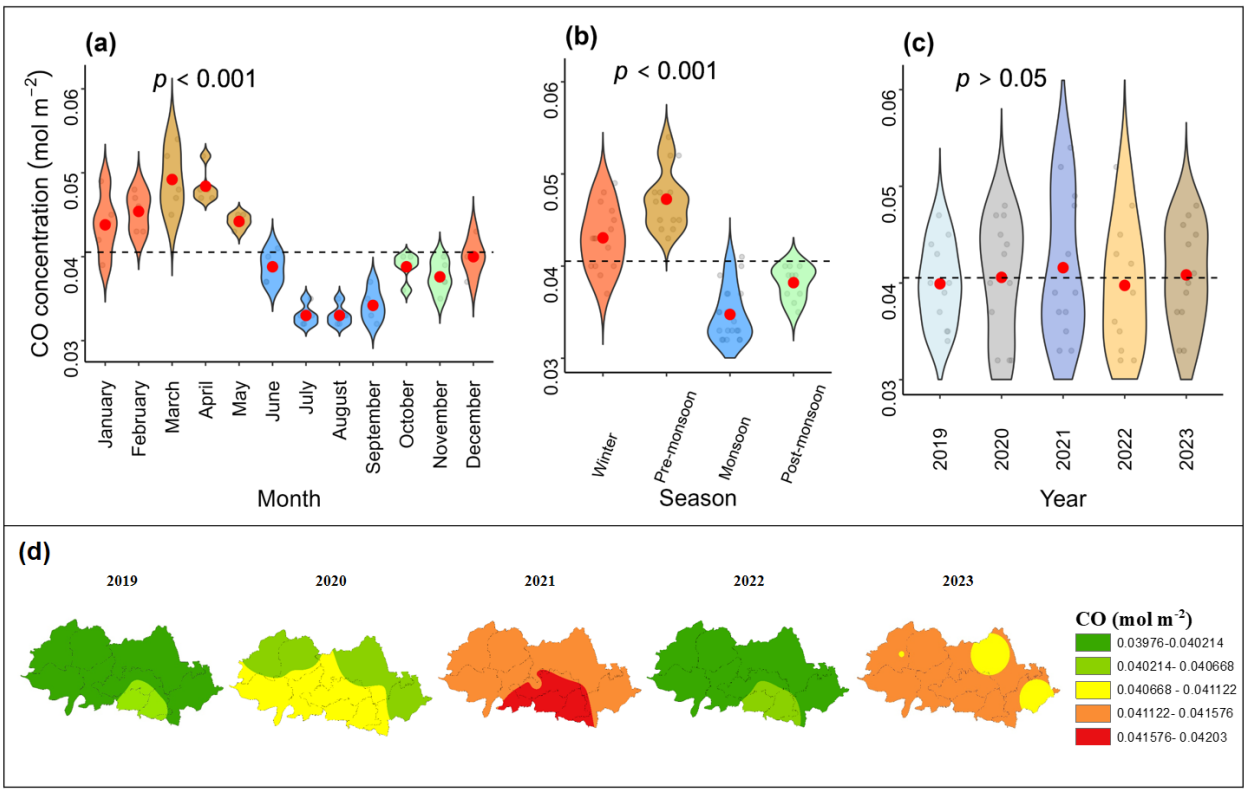

Fig. 5 Variations of CO concentration for the respective months (**a**), seasons (**b**), years (c), and spatial patterns of CO concentration (**d**) over the study area for the period 2019-2023. Figure descriptions are the same as those in Fig. 3, but for the CO concentration.

O_3 concentrations

The highest (lowest) monthly O_3 concentrations were 0.129 mol m^{-2} (0.114 mol m^{-2}) observed during April (January) (Fig. 6a). The O_3 concentrations were highest in the pre-monsoon (0.127 mol m^{-2}) and lowest in winter (0.117 mol m^{-2}) (Fig. 6b). The variations in O_3 concentrations showed significant differences for both monthly and seasonal changes (both $p < 0.01$). However, O_3 concentrations increased (ranging between 0.118 mol m^{-2} in 2019 and 0.125 mol m^{-2} in 2022), and the yearly variations in O_3 concentrations showed no significant differences (Fig. 6c, $p > 0.05$). Spatial patterns revealed that O3 concentrations varied across the entire study area (Fig. 6d). The lowest levels were observed in 2019, when concentrations were comparatively low throughout the region, while the highest occurred in 2022, when elevated concentrations predominated across the study area.

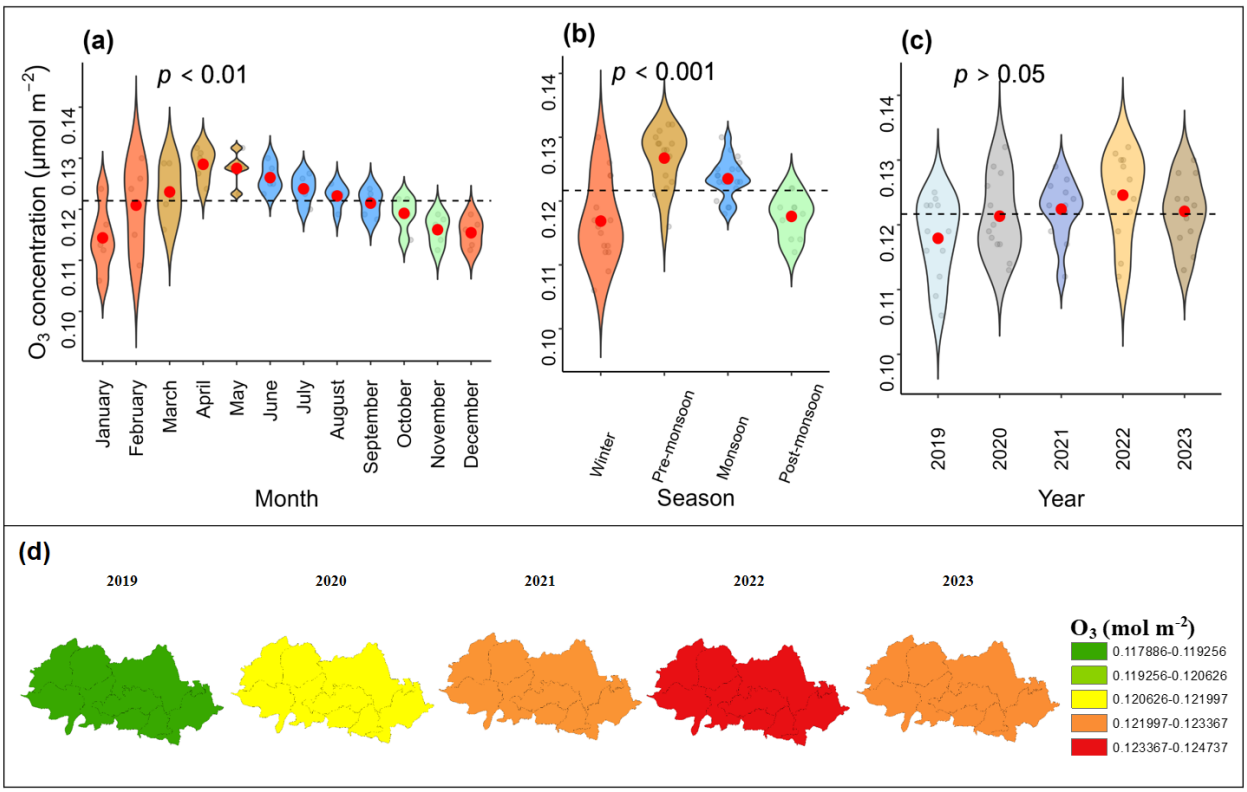

Fig. 6 Variations of O_3 concentration for the respective months (**a**), seasons (**b**), years (**c**), and spatial patterns of O_3 concentration (**d**) over the study area for the period 2019-2023. Figure descriptions are the same as those in Fig. 3, but for the O_3 concentration.

$PM_{2.5}$ concentrations

For $PM_{2.5}$ concentrations, significant variations were observed for monthly and seasonal variations (Fig. 7a & 7b, both $p < 0.001$); however, no significant variation was observed in annual changes (Fig. 7c, $p > 0.05$). Monthly data revealed that $PM_{2.5}$ concentrations peaked in May (45.1 µg/m³), while the lowest concentrations were observed in November (18.9 µg/m³). In terms of seasons, the pre-monsoon season experienced the highest average concentration of 40.74 µg/m³, while the post-monsoon season exhibited the lowest level at 20.60 µg/m³. Yearly, the highest $PM_{2.5}$ concentration (33.1 µg/m³) was observed in 2023, while the lowest (27.7 µg/m³) was recorded in 2019 (Fig. 7c). The analysis of the spatial variation over the five study years demonstrated differences in $PM_{2.5}$ concentrations across the regions of the study area. The southern region generally exhibited higher concentrations of PM2.5 than the northern region over the five years, with the highest concentrations observed in 2023 (Fig. 7d).

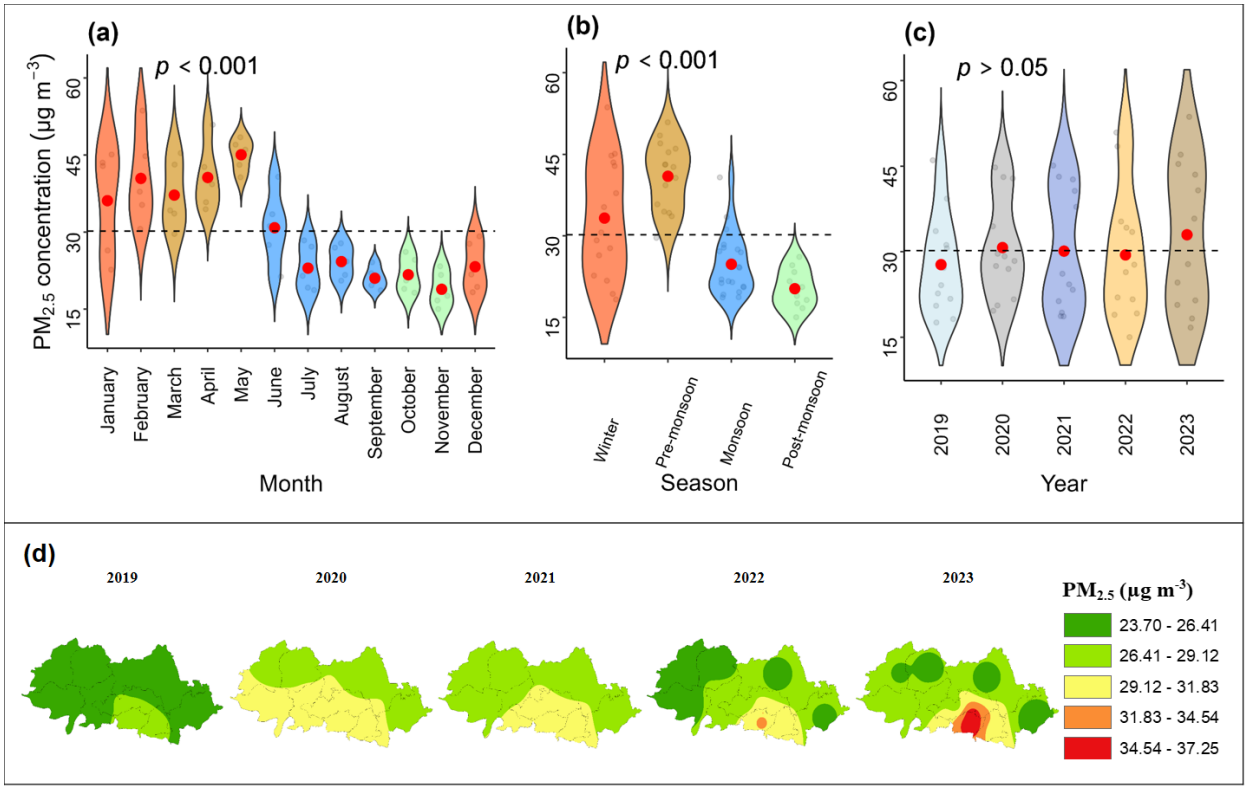

Fig. 7 Variations of $PM_{2.5}$ concentration for the respective months (**a**), seasons (**b**), years (**c**), and spatial patterns of $PM_{2.5}$ concentration (**d**) over the study area for the period 2019-2023. Figure descriptions are the same as those in Fig. 3, but for the $PM_{2.5}$ concentration.

NDVI

As for the NDVI values, significant variations were evident in monthly (Fig. 8a) and seasonal (Fig. 8b) NDVI (both $p < 0.001$), while no notable yearly differences were observed (Fig. 8c, $p > 0.05$). The highest and lowest NDVI values were recorded in October (0.693) and June (0.432). Seasonally, NDVI values increased from winter (0.497), to monsoon (0.525), pre-monsoon (0.557), and post-monsoon (0.656). Over the five years, 2019 had the highest NDVI value (0.574), while 2022 had the lowest (0.52) (Fig. 8c). The northeastern parts consistently showed higher NDVI values, indicating more vigorous vegetation compared to other regions of the study area (Fig. 8d).

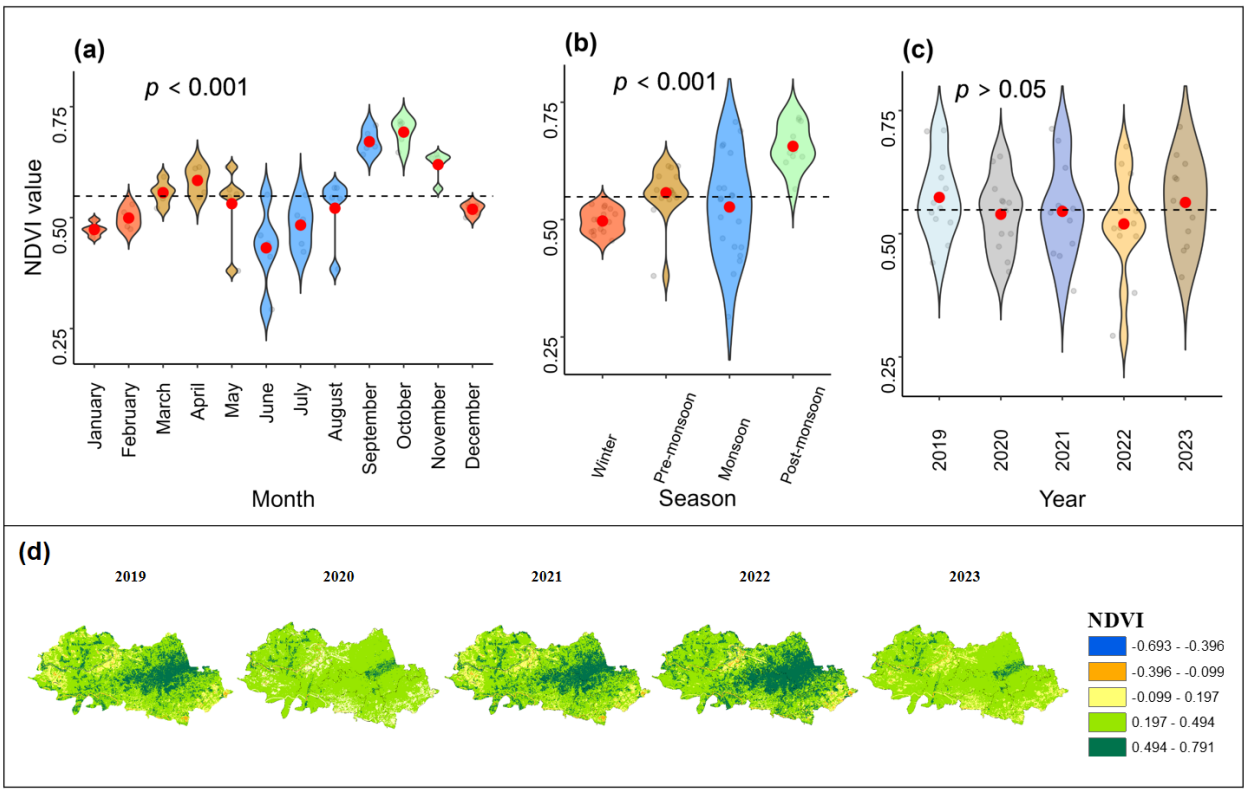

Fig. 8 Variations of NDVI values for the respective months (**a**), seasons (**b**), years (**c**), and spatial patterns of NDVI values (**d**) over the study area for the period 2019-2023. Figure descriptions are the same as those in Fig. 3, but for the NDVI values.

Relationships between vegetation greenness and air pollutants

Examination of the relationships between vegetation greenness and air pollutants revealed that NDVI showed a negative correlation with the five studied air pollutants (Fig. 9), with significant negative correlations observed between NDVI and NO_2 (r = -0.41, $p < 0.05$) and between NDVI and $PM_{2.5}$ (r = -0.36, $p < 0.05$). $PM_{2.5}$ exhibited significant positive correlations with NO_2 (r = 0.39), CO (r=0.76), SO_2 (r = 0.35), and O_3 (r=0.31) (all $p < 0.05$). In addition, the relationships between SO_2 and NO_2 (r = 0.45), SO_2 and CO (r = 0.45), and CO and NO_2 (r = 0.50) were found to be significantly positive (Fig. 9; all $p < 0.05$).

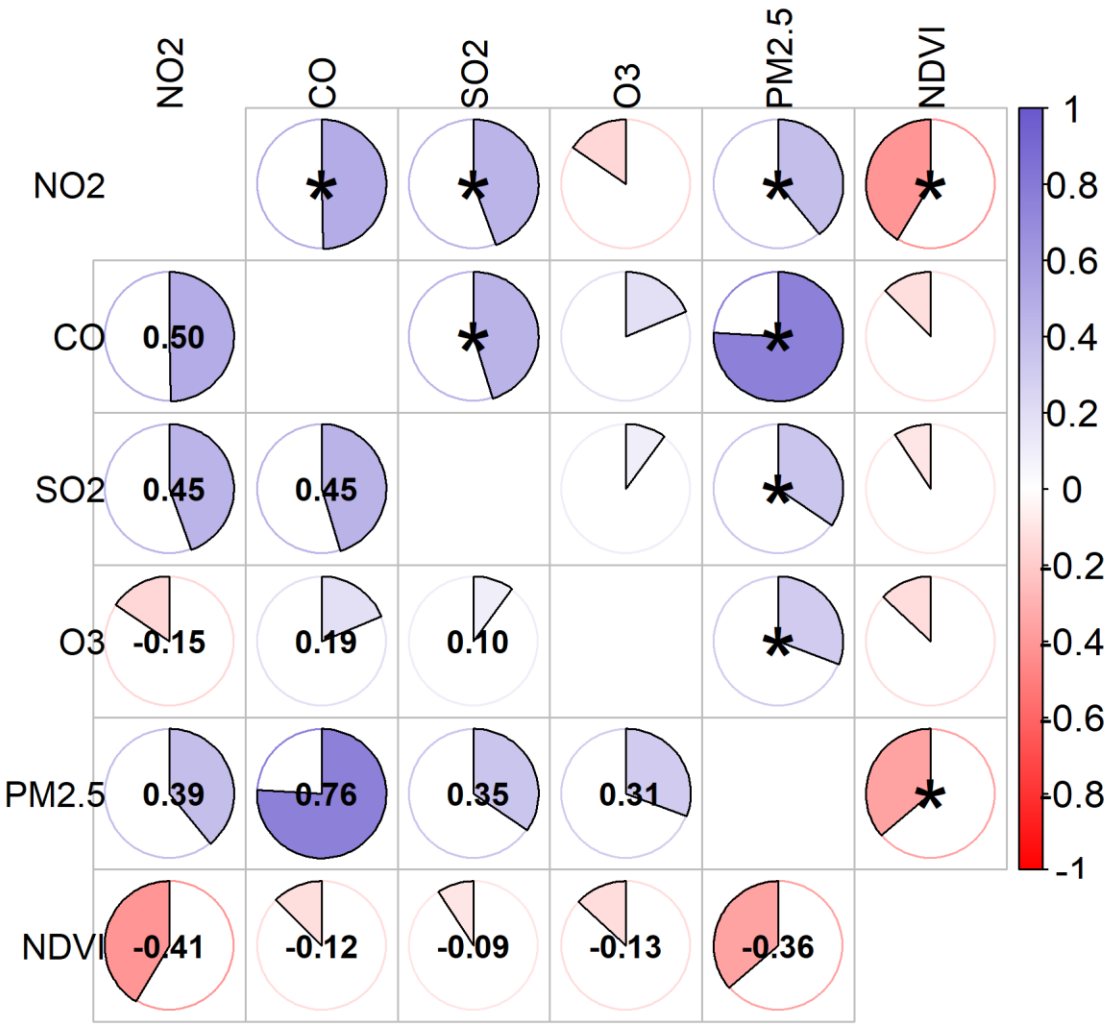

Fig. 9 Correlation matrix illustrating Pearson's correlation coefficients between selected air pollutants and NDVI. In the upper triangle, significant correlations ($p < 0.05$) are marked with asterisks (*), while insignificant correlations ($p > 0.05$) are left blank. The lower triangle displays the correlation coefficients. Correlations are represented using pie chart symbols with a color gradient ranging from slate blue ($r = +1$, strong positive correlation) to white ($r = 0$, no correlation) to red ($r = -1$, strong negative correlation).

Discussion

The study provides a comprehensive understanding of the relationship between vegetation health and air quality in the region by analyzing data on five major air pollutants and their impact on vegetation greenness. The analysis focuses on the concentrations of pollutants, including NO2, CO, O3, SO2, and PM2.5, from 2019 to 2023. These findings highlight the complex interactions between air pollution and vegetation, while also revealing critical patterns that can inform both environmental monitoring and policy-making.

The findings demonstrate that concentrations of pollutants exhibit substantial seasonal variations, with NO2 and SO2 reaching their maximum concentrations during winter, while O3 and CO levels remain relatively stable throughout the year. The findings of this research are consistent with those of previous studies (Jion et al., 2024; Saha *et al*., 2024), further validating the observed trends in air pollution and vegetation dynamics. For instance,

Jion *et al.* (2024) reported that NO_2 concentrations in Rajshahi and SO_2 concentrations in Dhaka peaked during winter due to emissions from brick kilns, brickfields, and biomass burning. Similarly, this study observed that $PM_{2.5}$ concentrations reached their highest levels during winter, particularly in January, corroborating the seasonal emissions patterns highlighted in Jion *et al.* (2024). This consistency highlights the substantial impact of colder months on air quality, which is driven by increased emissions and reduced atmospheric dispersion.

The seasonal vegetation dynamics observed in this study also align with findings from previous research (Fattah and Morshed 2022; Das *et al.* 2023). Using NDVI as an indicator of vegetation greenness, the study found that vegetation cover was lowest during winter and peaked during the monsoon season. These patterns are consistent with the findings of Fattah & Morshed (2022), who reported a strong positive association between NDVI and rainfall, emphasizing the critical role of rainfall in sustaining vegetation. Moreover, results of this study demonstrate a robust positive relationship between NDVI values and the monsoon season, further supporting the observations of Fattah & Morshed (2022).

The results of this study show that $PM_{2.5}$ levels reach their highest point during winter, particularly in January, due to reduced atmospheric dispersion and increased emissions from industrial and heating-related activities. Seasonally, winter exhibits the highest $PM_{2.5}$ concentrations, while pre-monsoon and monsoon seasons show lower levels due to heavy rainfall removing particulate matter from the air. The post-monsoon season experiences a gradual increase in PM2.5 as emissions rise and atmospheric conditions become less favorable for dispersion. There are changes in the yearly trends from 2019 to 2023, with higher average concentrations in some years.

In terms of the relationship between air pollutants and vegetation cover, this study revealed a significant inverse association between $PM_{2.5}$ concentrations and NDVI, indicating that particulate matter has an adverse effect on vegetation. This finding aligns with the study by Kulsum & Moniruzzaman (2021), which also reported a significant negative correlation between $PM_{2.5}$ levels and vegetation cover in the Greater Dhaka region. Consistent with the findings of Kulsum & Moniruzzaman (2021), this study also found the highest $PM_{2.5}$ concentrations during winter and the lowest in monsoon. This shared pattern highlights the detrimental impact of particulate matter on plant health and underscores the role of vegetation in mitigating air pollution (Su *et al*., 2022).

This study identified inverse relationships between NDVI and SO_2, CO, and O_3, though these associations were not statistically significant. This finding contrasts with the stronger and significant negative correlations observed for NO_2 and $PM_{2.5}$, suggesting that particulate matter and NO_2 have a greater influence on vegetation health compared to other gaseous pollutants. These findings align with a recent study conducted across major South Asian cities (Saha *et al*., 2024), which reported that six major air pollutants had a negative impact on vegetation greenness. NO_2, primarily emitted from industrial activities and combustion processes, can cause oxidative stress, damage plant tissues, and inhibit photosynthesis, reducing vegetation greenness. Similarly, SO_2 can enter plant cells through the stomata and disrupt physiological processes, further contributing to lower NDVI values. While CO is not directly harmful to plants, its presence often indicates urbanization and industrial activities, which can indirectly reduce vegetation cover through habitat loss and changes in land use. O_3, a well-documented phytotoxic pollutant, directly damages plant cells, reduces photosynthetic efficiency, and impairs overall vegetation health. These pollutants collectively act as stressors, particularly in areas with high concentrations, which can potentially inhibit vegetation growth. However, the weaker relationships observed for SO_2, CO, and O_3 in this study may suggest that their impacts on vegetation are more context-dependent or less direct than those of $PM_{2.5}$ and NO_2. Overall, the consistency between the findings of this study and those of previous studies reinforces the critical

importance of tackling air pollution to protect vegetation cover and maintain ecological balance. It also emphasizes the necessity for region-specific air quality management strategies to reduce the harmful impacts of particulate matter on plant health and environmental sustainability.

Conclusion

Understanding the interactions between air pollution and vegetation greenness is essential, as it provides valuable insights into ecosystem health, biodiversity conservation, and climate change mitigation. This study analyzed the patterns of five key pollutants (NO_2, SO_2, O_3, CO, and $PM_{2.5}$) and their relationships with vegetation greenness (NDVI) in Sylhet Sadar, Bangladesh, over a five-year period. Monthly and seasonal variations in NO_2, CO, O_3, and $PM_{2.5}$ concentrations were significant, with NO_2 peaking in winter and CO, O_3, SO_2, and $PM_{2.5}$ reaching their highest levels during the pre-monsoon season. Spatially, NO_2 concentrations were higher in the eastern part of the region, while SO_2 and $PM_{2.5}$ were elevated in the south. $PM_{2.5}$ and NO_2 exhibited the strongest negative correlations with NDVI, indicating their pronounced adverse effects on vegetation, driven by emissions from industrial activities, biomass burning, and reduced atmospheric dispersion in colder months. While SO_2, CO, and O_3 also exhibited inverse relationships with NDVI, these associations were not statistically significant, suggesting that their impacts on vegetation may be more indirect or context-dependent.

Additionally, positive correlations among the pollutants suggest overlapping emission sources, highlighting the necessity for integrated air quality management. This study highlights the critical necessity of targeted interventions, including air quality management and urban greening initiatives, to mitigate the adverse impacts of air pollution on vegetation health and promote sustainable urban development in rapidly growing cities. The study findings can inform local policymakers and environmental managers in devising strategies to enhance urban greenery and improve air quality, ultimately contributing to enhanced public health outcomes and fostering ecological sustainability.

DECLARATION

Authors' contributions Shithi Dhar Bristy: Conceptualization, methodology, data collection, formal analysis, writing-original draft, writing-review, and editing. **Md Lokman Hossain:** Formal analysis, writing-original draft, writing-review, and editing. **Md. Sabbir Ahmed Ruman:** Data collection, software. **Jannat Binte Jalal:** Data collection, software. **Derrick Y.F. Lai:** Writing-review and editing. **Pinaki Chowdhury:** Conceptualization, methodology, writing-review and editing, project administration, supervision, and funding acquisition.

Acknowledgement The satellite data used in this analysis were sourced from the European Union's Copernicus programme, implemented by the European Space Agency (ESA), and from the Land Processes Distributed Active Archive Center (LP DAAC), located at the U.S. Geological Survey (USGS) Earth Resources Observation and Science (EROS) Center. The authors are grateful to these institutions for making this data publicly available. M.L. Hossain was supported by the RGC of the Hong Kong SAR, China, through the RGC Postdoctoral Fellowship Scheme 2024/25 [Award Ref. No.: PDFS2425-4S05]. The authors thank the Research Cell of Noakhali Science and Technology University for the financial support they received to conduct the research.

Funding This work was supported by a research grant from the Research Cell, Noakhali Science and Technology University (NSTU/RC-ESDM/T-23/108).

Conflict of Interests: The authors declare that they have no competing interests or personal relationships that could appear to influence the work reported in this paper.

Ethical consideration: Not applicable

Data availability statement: This research utilized satellite data from the European Space Agency (ESA)/Copernicus programme and the NASA/USGS Land Processes DAAC (LP DAAC) at the USGS EROS Center.

References

Alam, M. Z., Armin, E., Haque, M., Kayesh, J. H. E., & Qayum, A. (2018). Air pollutants and their possible health effects at different locations in Dhaka City. *Journal of Current Chemical Pharmaceutical Sciences*, *8*(1), 111. https://doi.org/10.21767/2277-2871.1000111

Bangladesh Meteorological Department (BMD) (2025). Climate and weather data. https://live8.bmd.gov.bd/

Das, M. (2025). Bangladesh faces serious air pollution crisis. *The Lancet Oncology*, *26*(1), 18.

Das, A. C., Shahriar, S. A., Chowdhury, M. A., Hossain, M. L., Mahmud, S., Tusar, M. K., Ahmed, R., & Salam, M. A. (2023). Assessment of remote sensing-based indices for drought monitoring in the north-western region of Bangladesh. *Heliyon*, *9*(2).

Earth Engine Data Catalog. https://developers.google.com/earth-engine/datasets/

Eckhoff, R. K. (2009). Understanding dust explosions. The role of powder science and technology. *Journal of loss prevention in the process industries*, *22*(1), 105-116. https://doi.org/10.1016/j.jlp.2008.07.006

Fattah, M. A., & Morshed, S. R. (2022). Assessment of the responses of spatiotemporal vegetation changes to climatic variability in Bangladesh. *Theoretical and Applied Climatology*, *148*(1), 285-301. https://doi.org/10.1007/s00704-022-03943-7

Guo, L., Luo, J., Yuan, M., Huang, Y., Shen, H., & Li, T. (2019). The influence of urban planning factors on $PM_{2.5}$ pollution exposure and implications: A case study in China based on remote sensing, LBS, and GIS data. *Science of The Total Environment*, *659*, 1585-1596. https://doi.org/10.1016/j.scitotenv.2018.12.448

Gupta, P., & Follette-Cook, M. (2018). Converting AOD to $PM_{2.5}$: A statistical approach. NASA's Applied Remote Sensing Training Program. https://appliedsciences.nasa.gov/sites/default/files/D2P3_AODPMEx.pdf

Haque, M. N., Sharif, M. S., Rudra, R. R., Mahi, M. M., Uddin, M. J., & Abd Ellah, R. G. (2022). Analyzing the spatio-temporal directions of air pollutants for the initial wave of Covid-19 epidemic over Bangladesh: Application of satellite imageries and Google Earth Engine. *Remote Sensing Applications: Society and Environment*, *28*, 100862.

He, J., Gong, S., Yu, Y., Yu, L., Wu, L., Mao, H., Song, C., Zhao, S., Liu, H., Li, X., & Li, R. (2017). Air pollution characteristics and their relation to meteorological conditions during 2014–2015 in major Chinese cities. *Environmental pollution*, *223*, 484-496. https://doi.org/10.1016/j.envpol.2017.01.050

Hossain, M. L., & Li, J. (2021). NDVI-based vegetation dynamics and its resistance and resilience to different intensities of climatic events. *Global Ecology and Conservation*, *30*, e01768.

Hossain, M. L., Li, J., Lai, Y., & Beierkuhnlein, C. (2023). Long-term evidence of differential resistance and resilience of grassland ecosystems to extreme climate events. *Environmental Monitoring and Assessment*, *195*(6), 734.

Hou, S., Na Z., Lin T., Xiaofeng J., Yunyang L., and Xiuyi H. (2019). Pollution characteristics, sources, and health risk assessment of human exposure to Cu, Zn, Cd and Pb pollution in urban street dust across China between 2009 and 2018. *Environment International 128*, 430–37. https://doi.org/10.1016/j.envint.2019.04.046

Jion, M., & Islam, A. (2024). Identification of NO_2 and SO_2 pollution, trends and sources in Bangladesh. 7th International Conference on Civil Engineering for Sustainable Development (ICCESD), Bangladesh. http://www.iccesd.com/proc_2024/Papers/696.pdf

Kampa, M., & Castanas, E. (2008). Human health effects of air pollution. *Environmental Pollution 151* (2), 362–67. https://doi.org/https://doi.org/10.1016/j.envpol.2007.06.012

Kulsum, U., & Moniruzzaman, M. (2021). Quantifying the relationship of vegetation cover and air pollution: A spatiotemporal analysis of $PM_{2.5}$ and NDVI in Greater Dhaka, *Bangladesh. Jagannath Univ. J. Sci*, *7*(02), 54-63.

Kusuma, W. L., Chih-Da, W., Yu-Ting, Z., Hapsari, H. H., & Muhamad, J. L. (2019). $PM_{2.5}$ Pollutant in Asia—A comparison of metropolis cities in Indonesia and Taiwan. *International Journal of Environmental Research and Public Health*, *16*(24), 4924. https://doi.org/10.3390/ijerph16244924

Liu, C. (2002). Effect of $PM_{2.5}$ on AQI in Taiwan. *Environmental Modelling & Software*, *17*(1), 29–37. https://doi.org/10.1016/s1364-8152(01)00050-0

Liu, J. Y., Woodward, R. T., & Zhang, Y. J. (2021). Has carbon emissions trading reduced $PM_{2.5}$ in China?. *Environmental science & technology*, *55*(10), 6631-6643.

Majumder, A., Kundu, A., Hossain, M., Nayeem, A., & Islam, M. (2017). Particulate matter concentration dynamics in the air: Study from Sylhet City, Bangladesh. *The Jahangirnagar Review, Part II: Social Sciences*, Vol. XLI.

Murray, C. J., Aravkin, A. Y., Zheng, P., Abbafati, C., Abbas, K. M., Abbasi-Kangevari, M., & Borzouei, S. (2020). Global burden of 87 risk factors in 204 countries and territories, 1990–2019: a systematic analysis for the Global Burden of Disease Study 2019. *The lancet*, *396*(10258), 1223-1249.

Reig-Armiñana, J., Calatayud, V., Cerveró, J., García-Breijo, F., Ibars, A., & Sanz, M. (2004). Effects of ozone on the foliar histology of the mastic plant (*Pistacia lentiscus* L.). *Environmental Pollution*, *132*(2), 321–331. https://doi.org/10.1016/j.envpol.2004.04.006

Saha, M., Al Kafy, A., Bakshi, A., Nath, H., Alsulamy, S., Rahaman, Z. A., & Saroar, M. (2024). The urban air quality nexus: Assessing the interplay of land cover change and air pollution in emerging South Asian cities. *Environmental Pollution*, *361*, 124877.

Shaddick, G., Thomas, M. L., Mudu, P., Ruggeri, G., & Gumy, S. (2020). Half the world's population are exposed to increasing air pollution. *NPJ Climate and Atmospheric Science*, *3*(1), 23.

Su, T. H., Lin, C. S., Lu, S. Y., Lin, J. C., Wang, H. H., & Liu, C. P. (2022). Effect of air quality improvement by urban parks on mitigating $PM_{2.5}$ and its associated heavy metals: A mobile-monitoring field study. *Journal of Environmental Management*, *323*, 116283.

Tiwari, A., Vivian-Smith, A., Ljung, K., Offringa, R., & Heuvelink, E. (2012). Physiological and morphological changes during early and later stages of fruit growth in *Capsicum annuum*. *Physiologia Plantarum*, *147*(3), 396–406. https://doi.org/10.1111/j.1399-3054.2012.01673.x

Tuli, R. D., Rashid, K. J., Islam, M. M., Sobhan, M., Islam, S. T., Mondal, K. P., Talukder, B., & Mondal, A. M. (2025). Impact of climatic parameters on spatiotemporal variation of air pollutants across Bangladesh. *Urban Climate*, *59*, 102263.

Wei, J., Li, Z., Lyapustin, A. et al. First close insight into global daily gapless 1 km $PM_{2.5}$ pollution, variability, and health impact. *Nat Commun 14*, 8349 (2023). https://doi.org/10.1038/s41467-023-43862-3

World Health Organization (WHO). (2022). Ambient (outdoor) air pollution. https://www.who.int/news-room/fact-sheets/detail/ambient-(outdoor)-air-quality-and-health

Yan, S., Hui, C., Ying C., Chengzhen W., Tao H., & Hailan F. (2016). Spatial and temporal characteristics of air quality and air pollutants in 2013 in Beijing. *Environmental Science and Pollution Research*, *23*(14), 13996–7. https://doi.org/10.1007/s11356-016-6518-3

Zhang, G., Xu, H., Wang, H., Xue, L., He, J., Xu, W., Qi, B., Du, R., Liu, C., Li, Z., Gui, K., Jiang, W., Liang, L., Yan, Y., & Meng, X. (2020). Exploring the inconsistent variations in atmospheric primary and secondary pollutants during the 2016 G20 summit in Hangzhou, China: implications from observations and models. *Atmospheric Chemistry and Physics*, *20*(9), 5391–5403. https://doi.org/10.5194/acp-20-5391-2020